

Structural properties of solid energetic materials: a van der Waals density functional study

G. Vaitheeswaran*, K. Ramesh Babu, N. Yedukondalu and S. Appalakondaiah

Advanced Centre of Research in High Energy Materials, University of Hyderabad, Prof. C. R. Rao Road, Gachibowli, Hyderabad 500 046, India

In the present work we have focused our attention towards the complete description of structural properties of energetic solids, namely inorganic azides, secondary explosives and oxidizers through density functional theory-based calculations. We find large deviations in structural parameters calculated with the standard exchange-correlation functional such as local density approximation and generalized gradient approximation (GGA). On the other hand, dispersion-corrected density functional of (GGA + G06) describes the crystal structure of the energetic solids with good accuracy. This leads to the fact that the dispersion-corrected density functionals are essential to describe the crystal structure and thereby the related physical and chemical properties of the energetic solids.

Keywords: Crystal structure, density functional theory, dispersion interactions, energetic solids.

Introduction

SOLID energetic materials find numerous applications as explosives and fuels in defence, space and civilian sectors¹. The performance characteristics of energetic materials can be assessed by looking at their sensitivity towards external stimuli and other properties such as detonation pressure and detonation velocity which solely depend upon the crystal density and crystal structure². Thus for any energetic system, the accurate crystal structure description is mandatory to assess the fundamental properties related to its performance. In general, the crystal structure of energetic materials consists of molecular units composed of a large number of atoms. These molecular units bind through weak dispersive or van der Waals interactions^{3,4}. As the energetic systems contain a large number of atoms and complex chemical bonding, simulation of these kinds of molecular solids is a continuous challenge.

Density functional theory (DFT) is a successful tool in simulating and predicting the physical and chemical properties of a wide spectrum of materials^{5,6}. In many cases the results obtained through DFT calculations are in reasonable agreement with experimental data. However,

most of the energetic materials have complicated crystal structures with weak intermolecular interactions and hence the investigation of different physical and chemical properties of energetic materials through DFT is really a challenging task⁷. Byrd *et al.*⁸ have applied DFT to predict the structural properties of various energetic materials at ambient conditions. However, the predicted lattice parameters had large errors relative to the experiments. This is due to the fact that the usual DFT-based exchange-correlation functionals obtained within the local density approximation (LDA) and generalized gradient approximation (GGA) are not accurate enough to describe the systems having very small electronic overlap between the constituent atoms. Nevertheless, DFT can predict the lattice parameters of the energetic materials that are in close agreement with experiments provided the exchange-correlation functionals are corrected to describe the weak intermolecular interactions⁹⁻¹⁴.

In this present study, we have considered three kinds of energetic materials, namely inorganic azides NaN_3 , $\text{Ca}(\text{N}_3)_2$, $\text{Sr}(\text{N}_3)_2$; secondary explosives nitromethane (CH_3NO_2), HMX ($\text{C}_4\text{H}_8\text{N}_8\text{O}_8$), FOX-7 ($\text{C}_2\text{H}_4\text{N}_4\text{O}_4$) and oxidizers LiNO_3 , NaNO_3 and KNO_3 . The motivation behind choosing these three categories is the following: inorganic azides can be used as gas generators and also they are potential precursors to synthesize polymeric nitrogen, which is considered to be an ultimate green high-energy density material¹⁵. On the other hand, the secondary explosives are highly energetic systems and are used in war heads¹⁶. Oxidizers are oxygen-rich solids that decompose at moderate-to-high temperatures liberating oxygen gas¹⁷. The concentration of oxygen within an explosive or oxidizer is represented by a term known as 'oxygen balance', which is an important parameter for identifying its potential as an explosive or oxidizer. In general, the secondary explosives like HMX (-21.62%), and RDX ($\text{C}_3\text{H}_6\text{N}_6\text{O}_6$) (-21.6%) have oxygen deficiency and hence it is necessary to bind an oxidizer to the explosive¹⁸. The alkali metal nitrates LiNO_3 , NaNO_3 and KNO_3 can act as oxidizers with positive oxygen balance 58.1%, 47.1% and 39.6% respectively. They find applications as fertilizers, pyrotechnical compositions, and industrial explosives and in black powder¹⁸. To the best of our knowledge the complete description of the crystal structure

*For correspondence. (e-mail: gvsp@uohyd.ernet.in)

of these energetic materials is not presented in detail at the *ab initio* level. Hence we focused our attention towards the description of the crystal structure of these energetic solids by recently developed density functional methods. The remainder of the article is organized as follows: in the next sections we discuss the computational details followed by results and discussion. In the final section we give a brief conclusion of the present study.

Computational details

DFT calculations were performed with the Cambridge Sequential Total Energy Package (CASTEP) program using Vanderbilt-type ultrasoft pseudopotentials and a plane wave expansion of the wave functions^{19,20}. The crystal structures were relaxed using the Broyden, Fletcher, Goldfarb and Shannon (BFGS) method²¹. Exchange-correlation (XC) potential of Ceperley and Alder²², parameterized by Perdew and Zunger²³ (CA-PZ) in LDA and also GGA in Perdew–Burke–Ernzerhof (PBE)²⁴ were used. The Monkhorst–Pack scheme *k*-point sampling was used for integration over the Brillouin zone²⁵. The plane wave cut-off energy and *k*-point grid of 520 eV and $5 \times 8 \times 5$ *k*-point mesh for NaN₃ and 410 eV and $3 \times 3 \times 4$ for Ca(N₃)₂, Sr(N₃)₂ were used. The plane wave cut-off energy and *k*-point grid of 650 eV, $6 \times 5 \times 4$, 540 eV, $5 \times 2 \times 3$ and 520 eV, $5 \times 5 \times 3$ were used for nitromethane, HMX and FOX-7 respectively. Whereas for LiNO₃, NaNO₃ and KNO₃, the plane wave cut-off and *k*-point grid of 700 eV and $6 \times 6 \times 6$ for (Li/Na)NO₃ and $5 \times 3 \times 4$ for KNO₃ were used. In the geometry relaxation, the self-consistent convergence on the total energy is 5×10^{-6} eV/atom and the maximum force on the atom is found to be 0.03 eV/atom.

Dispersion corrections to DFT

Non-covalent forces such as van der Waals (vdW) interactions are crucial for the formation, stability and function of molecules and materials. The correct long-range interactions, for example, interactions in the case of separated molecules, are absent from all popular local-density and gradient-corrected XC functionals of DFT. To treat these interactions efficiently, there exists a variety of hybrid, semi-empirical solutions that introduce damped atom-pairwise dispersion corrections of the form C_6R^{-6} in the DFT formalism. The most well-known schemes were put forward by Grimme (GGA + G06)²⁶. According to the semi-empirical dispersion correction approach, the total energy of the system can be expressed as

$$E_{\text{total}} = E_{\text{DFT}} + E_{\text{Disp}},$$

where

$$E_{\text{Disp}} = s_i \sum_{i=1}^N \sum_{j>i}^N f(S_R R_{ij}^0, R_{ij}) C_{6,ij} R_{ij}^{-6}.$$

Here $C_{6,ij}$ is called dispersion coefficient between any atom pair *i* and *j*, which solely depends upon the material and R_{ij} is the distance between the atoms *i* and *j* respectively. Differences between DFT exchange-correlation functionals in the description of short to medium-range dispersion interaction are taken into account by a suitable modification of the correction potential through the parameters S_R .

Results and discussion

Inorganic metal azides

Sodium azide crystallizes in monoclinic structure with *C2/m* space group and contains two formula units per unit cell ($z = 2$)²⁷, while both Ca(N₃)₂ and Sr(N₃)₂ are isomorphic²⁸ and crystallize in orthorhombic structure²⁹, with eight formula units per cell ($z = 8$). The equilibrium crystal structure of the metal azides is achieved using three different functional, namely LDA (CA-PZ), GGA (PBE) and GGA + G06. The optimized crystal structures within GGA + G06 functional are shown in Figure 1. The optimized lattice parameters of the three azide systems are shown in Table 1. The computed crystal volume is underestimated by 9.5% for NaN₃, 3.8% for Ca(N₃)₂ and 3.9% for Sr(N₃)₂ in the CA-PZ-based computation. Whereas the PBE volume is overestimated by 7.9% for NaN₃, 7.9% for Ca(N₃)₂ and 8.5% for Sr(N₃)₂ respectively. The errors in computed equilibrium volume can be attributed to the fact that both functionals are inadequate to treat the weak dispersive forces present between the azide ions. The theoretical equilibrium volume calculated with GGA + G06 functional is underestimated by 0.08% for NaN₃ and overestimated by 3.5% for Ca(N₃)₂ and Sr(N₃)₂ respectively. It can be clearly seen that the DFT corrected with van der Waals interactions describes well the crystal structure of the studied inorganic metal azide systems.

Table 1. Equilibrium structural parameters of inorganic metal azides NaN₃, Ca(N₃)₂ and Sr(N₃)₂ calculated within LDA, GGA and GGA + G06 functionals

Compound	Method	<i>a</i> (Å)	<i>b</i> (Å)	<i>c</i> (Å)	β°	<i>V</i> (Å ³)
NaN ₃	LDA	5.868	3.568	5.081	102.5	103.8
	GGA	6.446	3.748	5.473	110.3	123.9
	GGA + G06	6.217	3.647	5.229	104.7	114.7
	Expt ²⁷	6.211	3.658	5.323	108.4	114.8
Ca(N ₃) ₂	LDA	10.802	10.882	5.879	–	691.1
	GGA	11.537	11.148	6.028	–	775.3
	GGA + G06	11.229	11.074	6.002	–	746.4
	Expt ²⁸	11.620	10.920	5.660	–	718.2
Sr(N ₃) ₂	LDA	11.404	11.429	6.083	–	792.8
	GGA	12.283	11.706	6.229	–	895.5
	GGA + G06	11.842	11.650	6.191	–	854.1
	Expt ²⁹	6.941	6.569	11.315	–	824.9

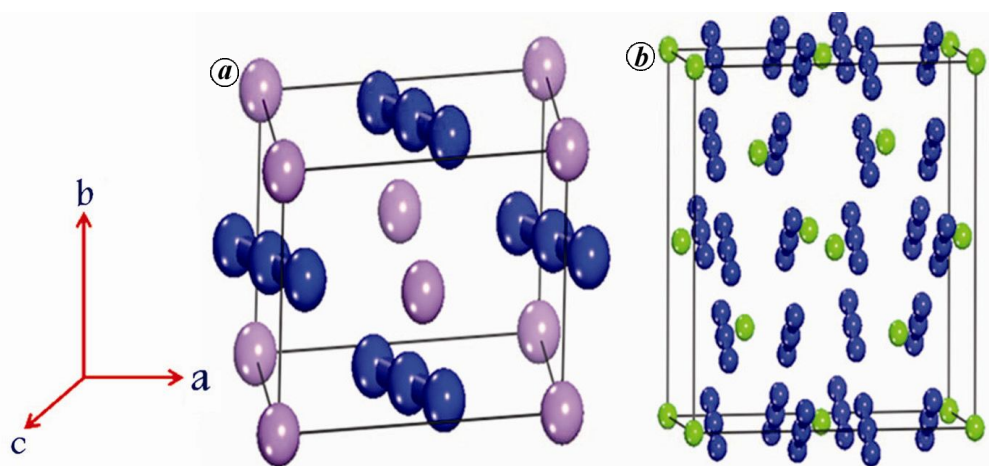


Figure 1. *a*, Optimized monoclinic crystal structure of NaN_3 using GGA + G06 functional. *b*, Optimized orthorhombic crystal structure of $\text{M}(\text{N}_3)_2$ ($\text{M} = \text{Ca}, \text{Sr}$) using GGA + G06 functional. Violet colour ball represents Na, green colour ball represents Ca or Sr and blue colour ball represents N atom respectively.

Table 2. Equilibrium structural parameters of secondary explosives calculated within LDA, GGA and GGA+G06 functionals

Compound	Method	$a(\text{\AA})$	$b(\text{\AA})$	$c(\text{\AA})$	β°	$V(\text{\AA}^3)$
Nitromethane	LDA	4.906	6.034	8.102	–	239.82
	GGA	5.471	6.731	9.102	–	334.59
	GGA + G06	5.193	6.287	8.577	–	280.01
	Expt ³⁰	5.183	6.235	8.518	–	275.31
HMX	LDA	6.377	10.299	8.507	124.63	459.81
	GGA	6.954	11.625	8.921	122.23	610.10
	GGA + G06	6.561	10.940	8.712	124.31	516.13
	Expt ³¹	6.540	11.050	8.700	124.30	519.39
FOX7	LDA	6.747	6.206	11.047	90.62	462.51
	GGA	7.226	7.777	11.648	92.02	654.22
	GGA + G06	6.998	6.516	11.305	91.23	515.45
	Expt ³²	6.941	6.569	11.315	90.55	515.89

Secondary explosives

Nitromethane (CH_3NO_2) is one of the simplest molecular crystals which belongs to the class of secondary explosives. It is a solid at low temperature of around 4.2 K and crystallizes in an orthorhombic structure with space group $P2_12_12_1$ (Figure 2)³⁰. 1,3,5,7-Tetranitro-1,3,5,7-tetraazacyclooctane (HMX, $\text{C}_4\text{H}_8\text{N}_8\text{O}_8$) is a secondary explosive belonging to the nitramine group and exists in four polymorphic phases – α , β , γ and δ . Of these, β -HMX is the stable phase at low and ambient temperatures, and crystallizes in monoclinic structure with two molecules per unit cell³¹. The experimental crystal structure of β -HMX is shown in Figure 2. FOX-7 (1,1-diamino-2,2-dinitroethene, $\text{C}_2\text{H}_4\text{N}_4\text{O}_4$) is a layered molecular crystal with monoclinic structure belonging to the space group $P2_1/n$ and contains four molecules (56 atoms) per unit cell³². In order to perform complete structural optimization of these three compounds, we have

started with the experimental lattice parameters as shown in Table 2. The obtained equilibrium lattice parameters are compared with experiments (Table 2). From Table 2, large overestimation with GGA (above 20%) and underestimation with LDA (around 10%) were observed for the three compounds. However, GGA + G06 functional improved the volumes as well as lattice parameters with a greater extent than standard DFT functionals. The computed values within GGA + G06 functional are in close agreement with experiments with a variation of 0.5–2%.

In the case of FOX-7, we found a large difference in the calculated and experimental volumes with both LDA (underestimated around 10%) and GGA (overestimated around 27% with PBE) functionals. Also, by comparing the three calculated lattice parameters of monoclinic FOX-7 unit cell, we have observed large deviation for b -lattice parameter compared to the other two parameters. This is because FOX-7 is a layered molecular system with the presence of weak vdW forces between the layers along b -axis of the lattice (Figure 2) which the usual density functionals are inadequate to account. This inconsistency between the experiments and calculated results from standard DFT functionals was overcome with vdW-corrected DFT functional GGA + G06. The calculated lattice parameter b is now in good agreement with the experimental value with 0.6% accuracy. In addition, the calculated volume also improves to a greater extent with 0.1% less compared with experiments.

Oxidizers

At room temperature, LiNO_3 (ref. 33) and NaNO_3 (ref. 34) crystallize in the trigonal structure with space group $R\bar{3}c$ and six formula units per unit cell ($z = 6$), whereas KNO_3 crystallizes in the primitive orthorhombic structure with space group $Pm\bar{c}n$ and four formula units per unit cell ($z = 4$)³⁵. For these materials also we have performed

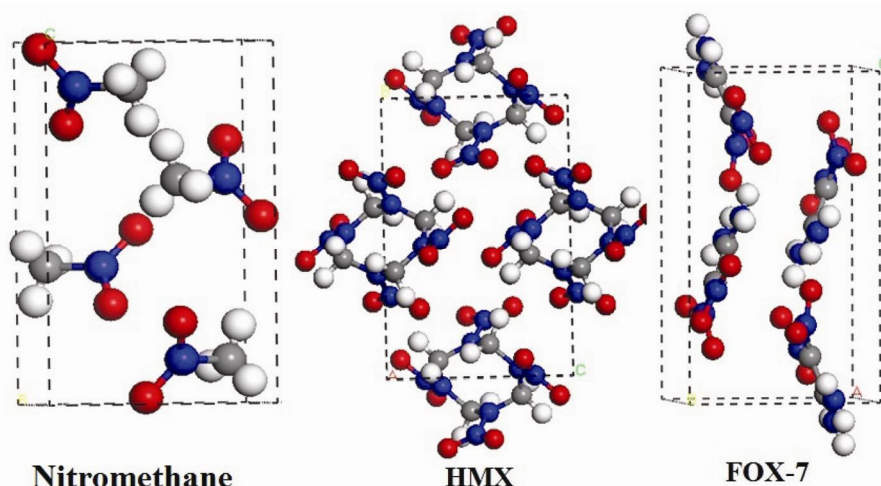


Figure 2. Crystal structure of secondary explosive systems. Grey, white, blue and red balls represent C, H, N and O atoms respectively.

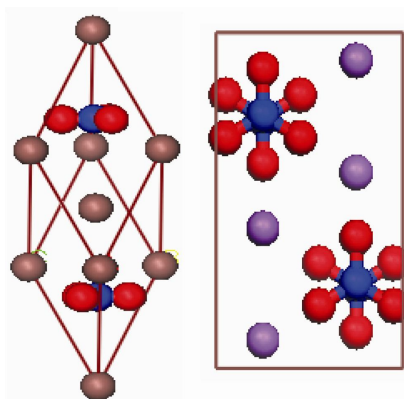


Figure 3. Equilibrium crystal structures of MeNO_3 ($\text{Me} = \text{Li}, \text{Na}$) (left) in Y - Z plane and KNO_3 (right) in X - Y plane. The brown, violet, red and blue colours represent Li or Na, K, O and N atoms respectively.

Table 3. Equilibrium structural parameters of oxidizers calculated within LDA, GGA and GGA + G06 functionals

Compound	Method	$a(\text{\AA})$	$b(\text{\AA})$	$c(\text{\AA})$	$V(\text{\AA}^3)$
LiNO_3	LDA	4.594	4.594	14.294	261.20
	GGA	4.791	4.791	15.514	308.35
	GGA + G06	4.752	4.752	15.227	297.73
	Expt ³³	4.692	4.692	15.215	290.08
NaNO_3	LDA	5.035	5.035	15.506	340.43
	GGA	5.195	5.195	17.091	399.42
	GGA + G06	5.175	5.175	16.593	384.91
	Expt ³⁴	5.070	5.070	16.822	374.49
KNO_3	LDA	5.241	8.859	5.877	272.91
	GGA	5.482	9.252	6.620	335.78
	GGA + G06	5.440	9.251	6.298	316.96
	Expt ³⁵	5.414	9.165	6.430	319.12

full structural optimization to get equilibrium crystal structure. The calculated volumes are underestimated by about 9–15% with LDA and overestimated about 5–6.5% with GGA-PBE. Our LDA values are consistent with pre-

vious theoretical calculations^{36,37} on KNO_3 . The obtained ground-state lattice parameters using standard LDA/GGA functionals show a large deviation from the experiments^{35–37}. Since the molecules within the unit cell bind through weak vdW forces and these non-local forces can be treated effectively with the semi-empirical dispersion correction methods, we have calculated the structural properties using GGA + G06 functional. However, the obtained volumes using G06 scheme deviate only by 0.7–2.8% and the equilibrium crystal structures within G06 are shown in Figure 3. Therefore, the GGA + G06 functional is successful in reproducing the structural properties of these molecular oxidizers in contrast to standard DFT functionals as shown in Table 3.

Conclusions

The present study explores the structural properties of energetic solids, namely inorganic azides, secondary explosives and oxidizers by performing the DFT calculations. We find that the crystal structure of the studied materials is well described by the dispersion-corrected functional with small errors of the order of below 2%. Whereas the usual density functionals such as LDA and GGA result in large errors of the order of above 6% on average for all the compounds. The present study concludes that the dispersion-corrected functionals are essential for proper description of the energetic solids.

1. Uddin, J., Barone, V. and Scuseria, G. E., Energy storage capacity of polymeric nitrogen. *Mol. Phys.*, 2006, **104**, 745–749.
2. Kamlet, M. J. and Jacobs, S. J., Chemistry of detonations: I. a simple method for calculating detonation properties of CHNO explosives. *J. Chem. Phys.*, 1968, **48**, 23–35.
3. Shimojo, F., Wu, Z., Nakano, A., Kalia, R. K. and Vashishta, P., Density functional study of 1,3,5-trinitro-1,3,5-triazine molecular crystal with van der Waals interactions. *J. Chem. Phys.*, 2010, **132**, 094106-8.

4. Sorescu, D. C. and Rice, B. M., Theoretical predictions of energetic molecular crystals at ambient and hydrostatic compression conditions using dispersion corrections to conventional density functionals (DFT-D). *J. Phys. Chem. C*, 2010, **114**, 6734–6738.
5. Jones, R. O. and Gunnarsson, O., The density functional formalism, its applications and prospects. *Rev. Mod. Phys.*, 1989, **61**, 689–746.
6. Payne, M. C., Teter, M. P., Allan, D. C., Arias, T. A. and Joannopoulos, J. D., Iterative minimization techniques for *ab initio* total-energy calculations: molecular dynamics and conjugate gradients. *Rev. Mod. Phys.*, 1992, **64**, 1045–1097.
7. Byrd, E. F. C. and Rice, B., *Ab initio* study of compressed 1,3,5,7-tetranitro-1,3,5,7-tetraazacyclooctane (HMX), cyclotrimethylenetrinitramine (RDX), 2,4,6,8,10,12-hexanitrohexaazaisowurztane (CL-20), 2,4,6-trinitro-1,3,5-benzenetriamine (TATB), and pentaerythritol tetranitrate (PETN). *J. Phys. Chem. C*, 2007, **111**, 2787–2796.
8. Byrd, E. F. C., Scuseria, G. E. and Chabalowski, C. F., An *ab initio* study of solid nitromethane, HMX, RDX, and CL20: successes and failures of DFT. *J. Phys. Chem. B*, 2004, **108**, 13100–13106.
9. Landerville, A. C., Conroy, M. W., Budzevich, M. M., Lin, Y., White, C. T. and Oleynik, I. I., Equations of state for energetic materials from density functional theory with van der Waals, thermal, and zero-point energy corrections. *Appl. Phys. Lett.*, 2010, **97**, 251908–3.
10. Ramesh Babu, K. and Vaitheeswaran, G., *Ab-initio* study of structural and vibrational properties of KN₃ under pressure. *Chem. Phys. Lett.*, 2012, **533**, 35–39.
11. Ramesh Babu, K. and Vaitheeswaran, G., Metal azides under pressure: an emerging class of high energy materials. *J. Chem. Sci.*, 2012, **124**, 1391–1398.
12. Appalakondaiah, S., Vaitheeswaran, G. and Lebègue, S., A DFT study on structural, vibrational properties, and quasiparticle band structure of solid nitromethane. *J. Chem. Phys.*, 2013, **138**, 184705-10.
13. Yedukondalu, N., Vikas, G. and Vaitheeswaran, G., Computational study of structural, electronic and optical properties of NH₄N₃. *J. Phys. Chem. C*, 2012, **116**, 16910–16917.
14. Yedukondalu, N., Vikas, G. and Vaitheeswaran, G., Pressure-induced structural phase transition in solid oxidizer KClO₃: a first principles study. *J. Chem. Phys.*, 2013, **138**, 174701-8.
15. Eremets, M. I., Popov, Yu. M., Trojan, I. A., Denisov, V. N., Boehler, R. and Hemley, R. J., Polymerization of nitrogen in sodium azide. *J. Chem. Phys.*, 2004, **120**, 10618–10623.
16. Akhavan, J., *The Chemistry of Explosives*, Royal Society of Chemistry, Cambridge, UK, 2004.
17. Steinhauser, G. and Klapotke, T. M., Green pyrotechnics: a chemists challenge. *Angew. Chem. Int. Ed. Engl.*, 2008, **47**, 3330–3347.
18. Meyer, M., Kohler, J. and Honburg, A., *Explosives*, Wiley, Germany, 2002, 5th edn.
19. Segall, M., Lindan, P., Probert, M., Pickard, C., Hasnip, P., Clark, S. and Payne, M. J., First-principles simulation: ideas, illustrations and the CASTEP code. *J. Phys.: Condens. Matter*, 2002, **14**, 2717–2744.
20. Vanderbilt, D., Soft self-consistent pseudopotentials in a generalized eigenvalue formalism. *Phys. Rev. B*, 1990, **41**, 7892–7895.
21. Kresse, G. and Furthmüller, J., Efficient iterative schemes for *ab initio* total-energy calculations using a plane-wave basis set. *Phys. Rev. B*, 1996, **54**, 11169–11186.
22. Ceperley, D. M. and Alder, B. J., Ground state of the electron gas by a stochastic method. *Phys. Rev. Lett.*, 1980, **45**, 566–569.
23. Perdew, J. P. and Zunger, A., Self-interaction correction to density-functional approximations for many-electron systems. *Phys. Rev. B*, 1981, **23**, 5048–5079.
24. Perdew, J. P., Burke, K. and Ernzerhof, M., Generalized gradient approximation made simple. *Phys. Rev. Lett.*, 1996, **77**, 3865–3868.
25. Monkhorst, H. J. and Pack, J., Special points for Brillouin-zone integrations. *Phys. Rev. B*, 1976, **13**, 5188–5192.
26. Grimme, S., Semi-empirical GGA-type density functional constructed with a long-range dispersion correction. *J. Comput. Chem.*, 2006, **27**, 1787–1799.
27. Pringle, G. E. and Noakes, D. E., The crystal structures of lithium, sodium and strontium azides. *Acta Crystallogr. B*, 1968, **24**, 262–269.
28. Gray, P., Chemistry of inorganic azides. *Q. Rev. Chem. Soc.*, 1963, **17**, 441–473.
29. Llewellyn, F. J. and Whitmore, F. E., The crystal structure of strontium azide. *J. Chem. Soc.*, 1947, **164**, 881–884.
30. Trevin, S. F., Prince, E. and Hubbard, C. R., Refinement of the structure of solid nitromethane. *J. Chem. Phys.*, 1980, **73**, 2996–3000.
31. Choi, C. S. and Boutin, H. P., A study of the crystal structure of β -cyclotetramethylene tetranitramine by neutron diffraction. *Acta Crystallogr. B*, 1970, **26**, 1235–1240.
32. Bemm, U. and Ostmark, H., 1,1-Diamino-2,2-dinitroethylene: a novel energetic material with infinite layers in two dimensions. *Acta Crystallogr. C*, 1997, **54**, 1997–1999.
33. Wu, X., Fronczek, F. R. and Butler, L. G., Structure of LiNO₃: point charge model and sign of the ⁷Li quadrupole coupling constant. *Inorg. Chem.*, 1994, **33**, 1363–1365.
34. Gonschorek, W., Schmahl, W. W., Weitzel, H., Mieke, G. and Fuess, H., Anharmonic motion and multipolar expansion of the electron density in NaNO₃. *Z. Kristallogr.*, 1995, **210**, 843–849.
35. Nimmo, J. K. and Lucas, B. W., A neutron diffraction determination of the crystal structure of phase potassium nitrate at 25 degrees C and 100 degrees C. *J. Phys.: Condens. Matter*, 1973, **6**, 201–211.
36. Lu, H. M. and Hardy, J. R., First principles study of phase transitions in KNO₃. *Phys. Rev. B*, 1991, **44**, 7215–7224.
37. Aydinol, M. K., Mantese, J. V. and Alpay, S. P., A comparative *ab initio* study of the ferroelectric behavior in KNO₃ and CaCO₃. *J. Phys.: Condens. Matter*, 2007, **19**, 496210-23.

ACKNOWLEDGEMENTS. We thank DRDO for funding through ACRHEM and CMSD, and the University of Hyderabad for computational facilities.